POAC'11
Montréal, Canada

Proceedings of the 21st International Conference on
Port and Ocean Engineering under Arctic Conditions
July 10-14, 2011
Montréal, Canada

POAC11-187

MODELLED BULK SALINITY OF GROWING FIRST-YEAR SEA ICE AND IMPLICATIONS FOR ICE PROPERTIES IN SPRING

Chris Petrich [1,2], Pat Langhorne [1], Hajo Eicken [2]

[1]Department of Physics, University of Otago, Dunedin, New Zealand

[2] Geophysical Institute, University of Alaska Fairbanks, Fairbanks, Alaska, USA

ABSTRACT

Sea ice brine volume controls many important seasonally varying properties of sea ice, such as its strength, dielectric properties, development of meltponds and surface albedo, and oil entrainment and migration to the ice surface. The brine volume fraction, which accounts for the bulk of the total porosity in first-year sea ice, depends primarily on the ratio of bulk salinity and ice temperature. While ice temperature and ice growth are readily modelled and can also be obtained from in-situ sensors or remote sensing, modelling or in-situ monitoring of bulk salinity has proved to be more elusive. We present a parameterization for the bulk sea ice salinity of growing ice as a function of ice growth rate that is based on concepts of natural convection in porous media (mushy layers). The results compare favourably with field data and more rigorous computational fluid dynamics simulations and provide a quantitative measure of increases in bulk salinity with increasing growth rate. The sensitivity of springtime bulk salinity and flexural strength is discussed based on a modelled case study for the Chukchi/Beaufort Sea region.

INTRODUCTION

Sea ice bulk salinity, the local mass-weighted salinity of ice crystals, air inclusions, and brine pockets, is a valued quantity because, in conjunction with temperature and sea ice density, it can be used to calculate the fractional brine volume. Compared with second-year and multiyear sea ice, first-year sea ice contains only a small fraction of air inclusions, allowing the brine volume to be used to calculate ice physical properties such as strength, permeability to fluid motion, optical extinction, and electromagnetic signatures (Petrich and Eicken, 2010). Unlike temperature, bulk salinity has the convenient property of decreasing during ice formation to reach a quasi-steady state after a few weeks (Nakawo and Sinha, 1981). Since the steady state lasts until the onset of melt, it is possible to estimate a wealth of ice properties at any given time during winter and early spring, provided the temperature history is known, and the bulk salinity profile has been determined at a representative time during the growth season. In fact, implicit in the description of bulk salinity developed in this manuscript is the conjecture that the bulk salinity profile itself can be estimated from the temperature history of the ice.

The latter notion is not new. For example, Nakawo and Sinha (1981) related data of steady-state bulk salinity, which they refer to as stable salinity, to growth rate with a functional relationship derived for a different segregation process. A similar approach was followed by Kovacs (1996)

and Petrich et al. (2006) who also fitted a function to the relationship between bulk salinity and growth rate, although they were guided in the selection of their fitting functions by subjectively apparent empirical relations. Here, we will introduce a steady-state bulk salinity parameterization that, in addition, provides a means of estimating how the steady-state bulk salinity would differ if, for example, brine viscosity, sea ice permeability or ocean salinity were different. Different fluid viscosities have been found in the presence of micro-algal activity (Nicols et al., 2005), systematic permeability differences may be related to difference in ice fabric (platelet, columnar, granular ice), and significantly different seawater salinities are observed for example in the Baltic Sea and Caspian Sea. By measuring steady-state bulk salinity and reversing the bulk salinity parameterization, it may be possible to make inferences on ice structure and growth conditions.

Our derivation of the bulk salinity parameterization is based on significant simplifications to the process of first-year sea ice growth and desalination as we understand it today (e.g. Petrich and Eicken, 2010). We derive a parameterization of the steady-state bulk salinity by parameterizing the process of desalination and integrating that process over time. The purpose of presenting the derivation of the steady-state bulk salinity parameterization is to provide hooks for subsequent improvements. Following the derivation, we will briefly present some predictions and comparisons with rigorous computational fluid dynamics simulations, and an application to modelling sea ice properties.

The most fundamental parameterization used in the following derivation is that of the brine volume flux inside sea ice. As laid out below, we assume that fluid motion is confined to ice near the ice–water interface where the porosity ϕ is larger than a characteristic porosity ϕ_c (Figure 1). This is in-line with observations of, for example, Cox and Weeks (1988) and Arrigo et al. (1993) who place ϕ_c at 0.05 and 0.07, respectively. There are two fundamentally different trains of thought as to why solute should be retained below a characteristic porosity for a particular set of growth conditions, i.e., percolation theory, and the critical Rayleigh number criterion in porous medium convection. Percolation theory predicts that, as a result of pore volume reduction, the pore space separates into discrete, disconnected clusters of pores (Golden et al., 1998, Petrich et al. 2006). Naturally, ions would be trapped in these clusters leading to steady-state bulk salinity. In a percolating medium of infinite size, the percolation transition, i.e. the appearance of a cluster of infinite size, is known to happen at a well-defined critical porosity that depends on the pore space geometry. On the other hand, in porous medium convection, the decreasing size of individual pores decreases the permeability to fluid motion, which eventually reduces the porous medium Rayleigh number below the critical Rayleigh number necessary for natural convection inside a porous medium (Notz and Worster, 2008). In this case, ions are trapped in a region that does not participate in natural convection during desalination, although the pore space could still be flushed by forced convection. While the distinction between these two mechanisms would have to be made experimentally, for the purpose of the present parameterization, the relevant observation is that brine movement and desalination come to a (near) halt at low porosity.

In the derivation of the parameterization described below, we consider the growth of columnar sea ice in quiescent conditions, and in the absence of air inclusions. Further, we assume that the growth rate is approximately constant at the desalination time scale of a few days to weeks during which a newly accreted ice layer is losing most of its salt due to desalination. This assumption would be applicable in particular in the dark of winter when temperature fluctuations are mostly driven by passing storm systems at the time scale of about a week, and are damped by a snow

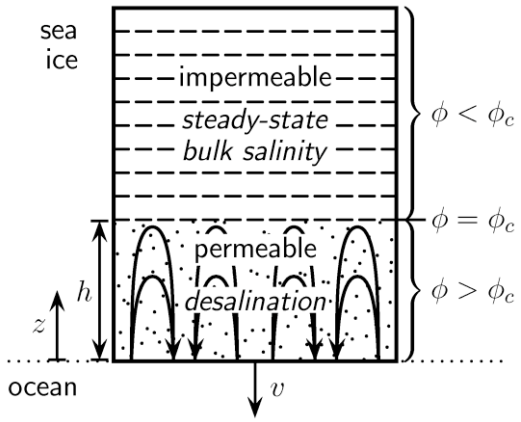

Figure 1. Cartoon of desalination.

cover. Further, we assume a linear dependence of the freezing point of brine on solute concentration, which is a good approximation in sea ice above the precipitation of mirabilite at about -8 °C (Petrich and Eicken, 2010), i.e., it is valid for the temperature range in which most of the desalination takes place. The parameterization will use solute concentration rather than salinity. In the case of small brine volume fractions typical for cold sea ice, ϕ, the relationship can be approximated by $\frac{S_{ice}}{S_0} \approx \frac{\rho_0}{\rho_i}\frac{C\phi}{C_0}$, where S_0, C_0 and ρ_0 are salinity, concentration and density of seawater, respectively, and S_{ice}, C, and ρ_i are bulk sea ice salinity, brine concentration, and density of freshwater ice, respectively.

DESALINATION PARAMETERIZATION

Description

Sea ice desalinates because brine in pores within the ice matrix is replaced with less saline fluid from the ocean. The bulk of desalination of growing sea ice takes place in the bottom few centimetres, and we assume for simplicity that a depth h can be defined over which desalination takes place at an appreciable rate, while desalination essentially ceases above h (Figure 1). In this model, h (m) is defined by a prescribed characteristic porosity ϕ_c (volume fraction). We present a method to determine h, which is related to the key characteristics of ice growth.

The porosity profile in the ice develops in response to natural convection and desalination. We parameterize the vertical flux that effects desalination in terms of the dimensionless Rayleigh number Ra as

$$w\phi = \begin{cases} \gamma_S \frac{\alpha}{h} Ra & \text{where } \phi > \phi_c \\ 0 & \text{where } \phi \le \phi_c \end{cases}, \qquad (1)$$

where γ_S is a dimensionless fitting constant, α is the thermal diffusivity of the ice (m^2/s), and $w\phi$ is the vertical volume flux (m/s), i.e. w (m/s) denotes the vertical interstitial velocity of brine. A constant γ_S is required since the Rayleigh number is a generic scaling parameter, leaving the interpretation of the magnitude of Ra dependent on the geometry and other particulars of the system under consideration. The porous medium Rayleigh number is defined as

$$\mathrm{Ra} = \frac{\Pi\, g\, \Delta\rho\, h}{\mu\alpha}, \tag{2}$$

where Π (m^2) is a characteristic permeability of the convecting system, g (m/s^2) is the acceleration due to gravity, μ (kg/(sm)) is the dynamic viscosity of brine, and $\Delta\rho$ (kg/m^3) is the density difference that drives motion (Worster, 1992). Ultimately, brine moves because of a hydrostatically unstable density configuration, so the density difference to be considered is that of seawater and brine at the level h inside the ice. This can be expressed in terms of the brine concentration gradient $\partial C / \partial z$ as

$$\Delta\rho = \frac{\partial\rho}{\partial C}\frac{\partial C}{\partial z} h, \tag{3}$$

where $\partial\rho / \partial C \approx 0.8$ is the dependence of brine density on solute concentration, and z is the vertical coordinate, positive being upward (Figure 1). The effect of temperature on brine density does not need to be accounted for explicitly given that, for the purpose of this development, brine is at the freezing temperature and in thermodynamic equilibrium with ice, i.e.

$$T = mC, \tag{4}$$

where T (°C) is the temperature of ice and brine, and m=–0.054 Km^3kg^{-1} is the slope of the liquidus. In general, the bulk solute concentration $C\phi$ in a one-dimensional system evolves in the absence of diffusion as

$$\frac{\partial C\phi}{\partial t} = -\frac{\partial w\phi C}{\partial z}, \tag{5}$$

where z (m) is the distance from the ice–ocean interface, and t (s) denotes time (Petrich et al., 2006). The differential can be separated into

$$\frac{\partial C\phi}{\partial t} = -w\phi\frac{\partial C}{\partial z} - C\frac{\partial w\phi}{\partial z}. \tag{6}$$

As a first-order approximation, we assume that the volume flux within $0 \le z \le h$ is independent of position, i.e. $\partial w\phi / \partial z = 0$ and therefore

$$\frac{\partial C\phi}{\partial t} = -w\phi\frac{\partial C}{\partial z}. \tag{7}$$

Finally, we assume that the ice growth rate, ocean and atmospheric heat flux change slowly at the time scale of desalination (i.e., a few days), and that the temperature profile is linear. In this case, the temperature profile in the ice can be assumed to be constant in time and space and written as

$$\frac{T}{T_0} = 1 + \frac{1}{T_0}\frac{\partial T}{\partial z} z, \tag{8}$$

where T_0 is the temperature at the ice–ocean interface. Hence, v (m/s) may be interpreted as either rate of movement of the ice–ocean interface (i.e., ice growth rate) in negative z-direction (Eulerian picture), or as rate of apparent movement of a fixed point inside the ice away from the interface, in positive z-direction (Lagrangian picture). Note that v is defined as $v>0$ for growing sea ice (Figure 1). This concludes the narrative of the components of the model, and we will proceed by deriving an explicit expression for the steady-state bulk salinity.

Solution

The governing equations of the model are solute mass conservation,

$$\frac{\partial C\phi}{\partial t} = -w\phi\frac{\partial C}{\partial z}, \tag{9}$$

with the parameterization of volume flux with $w\phi$ given by equations (1) and (2)

$$w\phi = \begin{cases} \gamma_S \dfrac{\Pi}{\mu} g \dfrac{\partial \rho}{\partial C} \dfrac{\partial C}{\partial z} h & \text{where } \phi > \phi_c \\ 0 & \text{where } \phi \le \phi_c \end{cases}, \tag{10}$$

and the assumption of a linear temperature and brine concentration profile

$$\frac{C}{C_0} = 1 + \frac{1}{C_0} \frac{\partial C}{\partial z} z, \tag{11}$$

where C_0 is the brine concentration of the ocean ($C_0 \approx 34$ kgm^{-3}). Further, the constitutive relationship between bulk concentration $C\phi$ and porosity is

$$\phi = \frac{C\phi}{C}. \tag{12}$$

For notational convenience we define a velocity scale

$$w_0 = \frac{\Pi}{\mu} g \frac{\partial \rho}{\partial C} C_0 \tag{13}$$

and a length scale

$$z_x = \left[\frac{1}{C_0} \frac{\partial C}{\partial z} \right]^{-1}. \tag{14}$$

Since the growth rate v is constant at the time scale of desalination, we can recast the solute mass conservation equation (9) into a differential equation for the bulk concentration profile. The passage of time is equivalent to a translation in space following

$$v = \frac{\partial z}{\partial t}, \tag{15}$$

and therefore (9) can be written as

$$\frac{1}{C_0} \frac{\partial C\phi}{\partial z} = -\frac{w\phi}{v} \frac{1}{C_0} \frac{\partial C}{\partial z}. \tag{16}$$

Further, substituting (10) for $w\phi$ and using Equations (13) and (14), in the region $\phi > \phi_c$, we get

$$\frac{1}{C_0} \frac{\partial C\phi}{\partial z} = -\frac{\gamma_s w_0}{v} \frac{h}{(z_x)^2}. \tag{17}$$

Integrating with respect to z, starting at z=0 with $C\phi = C_0$, we obtain a general expression for the bulk salinity at position $0 \le z \le h$ of

$$\frac{C\phi}{C_0} = 1 - \frac{\gamma_s w_0}{v} \frac{h}{(z_x)^2} z. \tag{18}$$

Desalination ceases at z=h, and we obtain the steady-state bulk concentration

$$\frac{(C\phi)_c}{C_0} = 1 - \frac{\gamma_s w_0}{v} \left(\frac{h}{z_x} \right)^2. \tag{19}$$

We will solve this equation for h/z_x. The brine concentration C_c at h is known from (11), i.e.

$$\frac{C_c}{C_0} = 1 + \frac{h}{z_x}, \tag{20}$$

where $(C_c - C_0)/C_0 = h/z_x$ is the reduced brine concentration at ϕ_c.

From the constitutive relationship (12) we therefore know

$$\frac{(C\phi)_c}{C_0} = \phi_c \frac{C_c}{C_0} = \phi_c\left(1 + \frac{h}{z_x}\right). \tag{21}$$

Hence, equation (19) can be rewritten as a quadratic equation

$$\phi_c\left(1 + \frac{h}{z_x}\right) = 1 - \frac{\gamma_s w_0}{v}\left(\frac{h}{z_x}\right)^2 \tag{22}$$

which can be recast in terms of h/z_x as

$$\frac{h}{z_x} = \frac{\phi_c}{2}\frac{v}{\gamma_s w_0}\left[-1 + \sqrt{1 + \frac{2(1-\phi_c)}{\phi_c^2}\frac{\gamma_S w_0}{v}}\right]. \tag{23}$$

The steady-state bulk sea ice concentration can be obtained from

$$\frac{(C\phi)_c}{C_0} = \phi_c\left(1 + \frac{h}{z_x}\right). \tag{24}$$

We remark at this point that the radicand in (23) is generally larger than 1 at common ice growth rates, which suggests the use of the limit for small growth rates,

$$\frac{h}{z_x} \approx \sqrt{\frac{(1-\phi_c)}{2}\frac{v}{\gamma_s w_0}}\,. \tag{25}$$

However, we will proceed by using Equation (23).

Flux at the ice–ocean interface

We postulate that the flux at the ice–ocean interface, $(w\phi)_0$ (m/s), is proportional to the volume flux within the sea ice effecting desalination, i.e. similar to (1),

$$(w\phi)_0 = \gamma_F \frac{\alpha}{h} Ra\,, \tag{26}$$

where γ_F is a dimensionless scaling constant, and with substitutions of Equations (13) and (14),

$$(w\phi)_0 = \gamma_F\ w_0 \frac{h}{z_x}\,. \tag{27}$$

Further, we note that the Rayleigh number defined in Equations (2) and (3) can be expressed as

$$Ra = \left(\frac{h}{z_x}\right)^2 \frac{w_0\ z_x}{\alpha}\,. \tag{28}$$

Free parameters

Unless stated otherwise, we will use the following parameters:
$\phi_c = 0.05$, $\gamma_s w_0 = 4.5\times10^{-8}$ ms^{-1}, $\gamma_F w_0 = 3.0\times10^{-7}$ ms^{-1},
where the choice of ϕ_c was inspired by Cox and Weeks (1988) and $\gamma_s w_0$ and $\gamma_F w_0$ are fitted to

RESULTS

Figure 2a shows the growth-rate dependence of the steady-state bulk solute concentration for different values of ϕ_c. The steady-state salinity increases with growth rate, i.e., based purely on the advective process included in this model, ice has the potential to desalinate most efficiently at low growth rates (however, in this case, h will be large, increasing the desalination time scale).

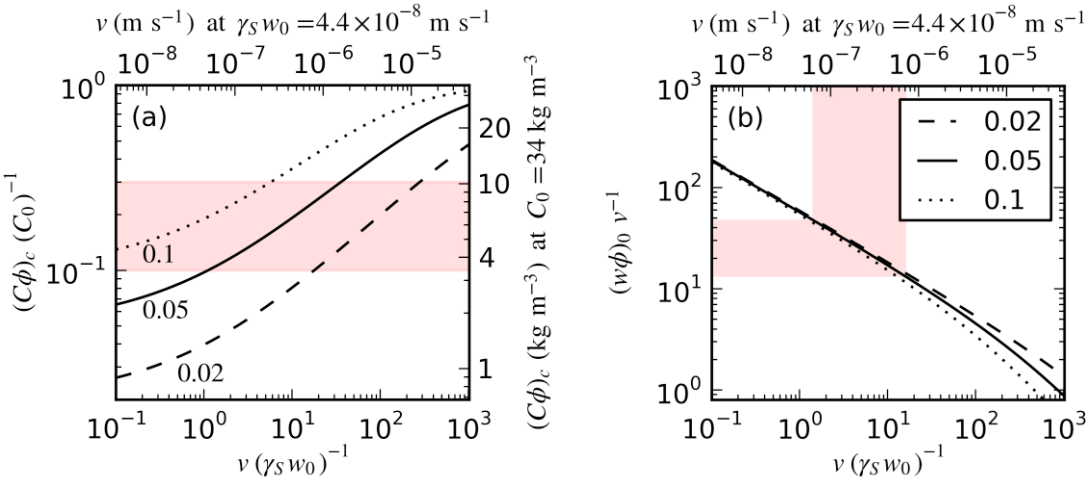

Figure 2. (a) Normalized steady-state bulk solute concentration as a function of normalized growth rate for different values of ϕ_c, and (b) relative flux at the ice–ocean interface. The labels at the right (figure a) and at the top (figures a and b) give example magnitudes for representative scaling constants. The shaded areas in (a) and (b) indicates the range of steady-state concentrations that is commonly observed in sea ice grown from ocean water. Note that the dependence of the flux at the ice–ocean interface on $\gamma_F w_0$ is not shown (Equation (27)).

The results show a strong dependence on ϕ_c, which can be partially compensated by tuning γ_s in the calibration process but may be of physical significance for ice of different fabric (see Discussion below). The ice–ocean interface flux shown in Figure 2b is, relative to the growth rate, highest at low growth rates, leading to an increased exchange of ocean water per unit of ice grown as the growth rate decreases. The expected volume of fluid exchanged between ocean and sea ice is of the order of 10 to 100 times the volume of ice grown. The flux at the ice–ocean interface is not directly dependent on ϕ_c, suggesting the distinction that the flux at the ice–ocean interface depends on the pore space near the ice–ocean interface, while the steady-state bulk concentration depends on the pore space at lower porosities, i.e. at ϕ_c in this parameterization.

The parameterizations of Equations (23)/(24) and (23)/(27) are compared with output from the Computational Fluid Dynamics (CFD) model of Petrich et al. (2006). In the CFD model, sea ice growth is treated rigorously in a domain that contains both liquid and porous sea ice. The fluid velocity in the liquid under the ice was left unconstrained and reached several centimetres per second. Unlike in the simulations of Petrich et al. (2006), the ice–ocean interface was left to evolve freely without assumptions about the porosity profile within the bottom-most cells containing ice. Results using either one of two permeability–porosity relationships are compared here, neither one of which (or any other part of the fluid dynamics simulations) contains an explicit cut-off comparable to the characteristic porosity ϕ_c. The parameterizations are

$$\Pi = \phi^3 \, 10^{-8} \ \mathrm{m}^2 \text{, and} \tag{33}$$

$$\Pi = \phi^2 \, 10^{-9} \ \mathrm{m}^2 . \tag{34}$$

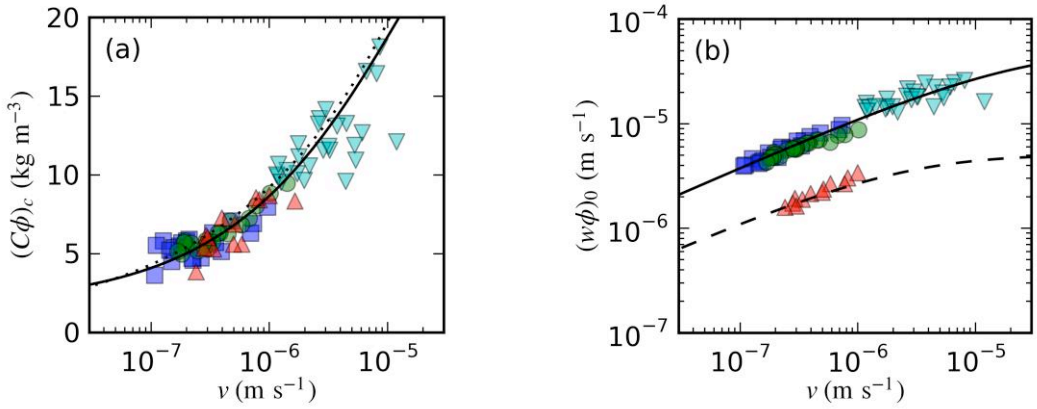

Figure 3. Comparison of the parameterization derived from this model (solid and dashed lines) with data from computational fluid dynamics simulations (markers) for (a) bulk salinity and (b) ice–ocean interface flux. Marker shapes and colours discriminate individual simulations. Upwards-pointing markers are from simulation using Equation (34), while the remaining simulations use Equation (33). Dashed line is for model results with $\gamma_s w_0 = 4.5\times10^{-9}$ ms^{-1}. For reference, the dotted line in (a) is an empirical fit given by Petrich et al. (2006).

In the CFD model ice was grown from an upper surface held at constant temperature. Simulation results using different domain sizes, grid sizes, and surface temperatures are compared with results from the present model in Figure 3. Looking past the scatter intrinsic to the fluid dynamics simulations in Figure 3a, the steady-state bulk solute concentration compare well in the CFD results and parameterization. In fact, they also agree well with a parameterization given by Petrich et al. (2006), which was found to agree with field measurements in Arctic landfast sea ice (Petrich and Eicken, 2010). Figure 3b shows that the interface flux depends on the interface permeability in the CFD simulations the same way as suggested by the parameterization. In particular, a reduction of the permeability at the ice–ocean interface ($\phi = 1$) by a factor 10 (Equation (34) vs. (33)) is reproduced by the parameterization if w_0 is reduced by a factor 10 (dashed line), which is expected from the linear dependence of w_0 on Π (Equation (13)).

DISCUSSION AND CONCLUSIONS

Desalination parameterization

Based on a highly idealized picture of desalination due to gravity drainage and an ad-hoc parameterization of fluid motion inside sea ice, we were able to arrive at parameterizations of the steady-state bulk solute concentration and of the flux at the ice–ocean interface. This picture is applicable to desalination during quiescent columnar growth. Processes that may be particularly relevant in highly dynamic environments, such frazil ice accumulation, wave pumping, and pressure suction, were not considered (e.g., Feltham et al., 2002). In addition we focused on gravity drainage as the dominant effect of desalination, omitting movement in response to brine expulsion from individual pockets in response to mechanical forces that should take place regardless of porosity (Notz and Worster, 2008). The most compelling argument for the utility of the derived parameterization is its agreement with rigorous CFD simulations, a selection of which were presented here. Unlike other parameterizations presented in the literature to-date, the current

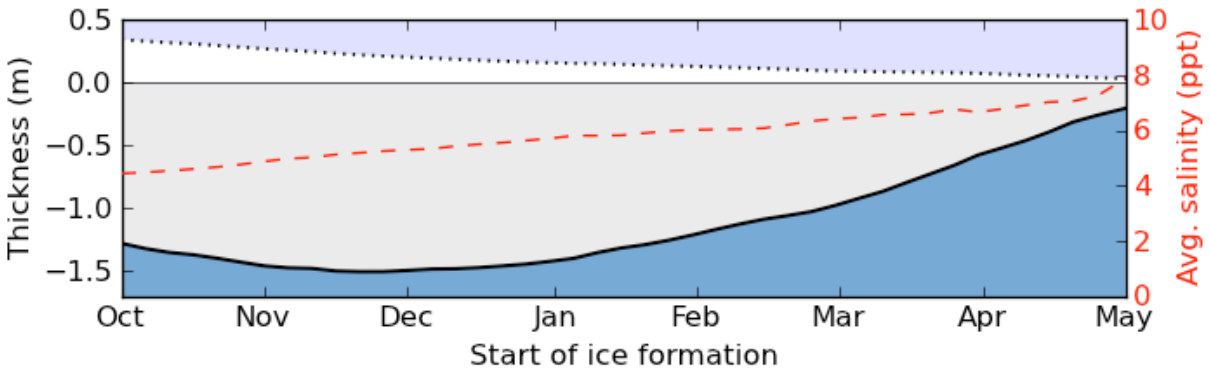

Figure 4. Modelled snow (dotted line), ice (solid line), and thickness-averaged bulk salinity (dashed line) of sea ice at the end of an average growth season in Barrow, Alaska (20 May).

parameterization is able to predict steady-state bulk salinity and the flux at the ice–ocean interface under a variety of conditions, including different ocean salinities, fluid viscosities and differences in crystal size and pore structure (through Π and ϕ_c). This capability may be useful to investigate the fabric-dependence of the pore space, such as those found in granular, columnar, and platelet ice.

Implications for ice strength

While the flexural strength of first-year sea ice is primarily a function of porosity, porosity depends on bulk salinity and temperature. Timco and Johnston (2002) estimated flexural strength as a function of ice temperature and bulk salinity. For temperatures above -5 °C, the strength at any given temperature is strongly dependent on bulk salinity and is approximately inversely proportional to bulk salinity. Based on the present model and 2000–2009 average temperature and precipitation data for Barrow, Alaska (71° N), we calculate the expected average bulk salinity of a slab of growing first-year sea ice as a function of the date of initial ice formation. Ice growth is simulated with a simple two-layer quasi-steady state thermal conduction model (one layer snow, one layer ice), neglecting solar radiation. The end-of-season ice conditions are evaluated on 20 May, at a time where ice temperatures can be expected to be anywhere above -7 °C and snow melt is just about to start. Figure 4 shows the expected end-of-season snow depth, ice thickness, and average bulk salinity. The relationship between ice age and thickness is non-linear, with ice starting to form at the end of November growing thickest. However, the average bulk salinity of growing first-year sea ice is linearly correlated with ice age, with the oldest ice exhibiting the lowest average bulk salinity. Note that this is not because older ice had more time to desalinate but rather because older ice had a larger fraction of the ice grow at a lower rate, which reduces bulk salinity. The average bulk salinity spans a range from just above 4 to just under 8 ppt, suggesting that the flexural strength of ice encountered at that time of year varies by a factor two, with the oldest ice being strongest, based on considerations of bulk salinity alone. These results can be transferred to floes taking into account spatial inhomogeneity, for example in response to snow depth variations, or refrozen cracks (Langhorne and Haskell, 2004; Petrich et al., 2007).

ACKNOWLEDGEMENTS

The parameterization was developed while CP was supported by a postdoctoral fellowship through the Foundation of Research, Science, and Technology, New Zealand. In-depth analysis

and comparison with computational fluid dynamics simulations were performed under support of an International Polar Year presidential postdoctoral fellowship of the University of Alaska Foundation. The constructive comments of the reviewer are gratefully acknowledged.

REFERENCES

Arrigo, K. R., Kremer, J. N., and Sullivan, C. W., 1993, A simulated Antarctic fast ice ecosystem, Journal of Geophysical Research – Oceans, 98(C4), 6929–6946.

Cox, G. F. N., W. F. Weeks, 1988, Numerical simulations of the profile properties of undeformed first-year sea ice during the growth season, Journal of Geophysical Research – Oceans, 93(C10), 12,449–12,460.

Feltham, D. L., M. G. Worster, and J. S. Wettlaufer, 2002, The influence of ocean flow on newly forming sea ice. Journal of Geophysical Research – Oceans, 107, 3009, doi:10.1029/2000JC000559.

Golden, K. M., S. F. Ackley, and V. I. Lytle, 1989, The percolation phase transition in sea ice, Science, 282(5397), 2238–2241.

Kovacs, A., 1996, Sea ice. Part I. Bulk salinity versus ice floe thickness, Cold Regions Research and Engineering Laboratory Report 96-7, 16 pp.

Langhorne, P. J., and T. G. Haskell, 2004, The flexural strength of partially refrozen cracks in sea ice. In Proceedings of the 14th International Offshore and Polar Engineering Conference, Toulon, France, 23–28 May 2004, 819–824.

Nakawo, M., and N. K. Sinha, 1981, Growth rate and salinity profile of first-year sea ice in the high Arctic, Journal of Glaciology, 27(96), 315–330.

Nichols, C. M., J. P. Bowman, and J. Guezennec, 2005, Effects of incubation temperature on growth and production of exopolysaccharides by an Antarctic sea ice bacterium grown in batch culture, Applied and Environmental Microbiology, 71(7), 3519–3523.

Notz, D., and M. G. Worster, 2008, In situ measurements of the evolution of young sea ice, Journal of Geophysical Research – Oceans, 113, C03001, doi:10.1029/2007JC004333.

Petrich, C. and H. Eicken, 2010, Growth, Structure and Properties of Sea Ice. In Thomas and Dieckmann (eds), Sea Ice, 2nd ed, Wiley–Blackwell, pp. 23–77.

Petrich, C., P. J. Langhorne, and Z. F. Sun, 2006, Modelling the interrelationships between permeability, effective porosity and total porosity in sea ice, Cold Regions Science and Technology, 44(2), 131–144. doi:10.1016/j.coldregions.2005.10.001.

Petrich, C., P. J. Langhorne, and T. G. Haskell, 2007, Formation and structure of refrozen cracks in land-fast first-year sea ice. Journal of Geophysical Research – Oceans, 112, C04006, doi:10.1029/2006JC003466.

Timco, G. W. and M. E. Johnston, 2002, Sea ice strength during the melt season. In: Ice in the environment: Proceedings of the 16th IAHR International Symposium on Ice. 6–12 December 2002, Dunedin, New Zealand, 187–193.

Worster, M. G., 1992, Instabilities of the liquid and mushy regions during solidification of alloys. Journal of Fluid Mechanics, 237, 649–669.